

MR imaging of renal cortical tumours: qualitative and quantitative chemical shift imaging parameters

Christoph A. Karlo · Olivio F. Donati · Irene A. Burger ·
Junting Zheng · Chaya S. Moskowitz · Hedvig Hricak ·
Oguz Akin

Received: 27 August 2012 / Revised: 31 October 2012 / Accepted: 1 December 2012 / Published online: 10 January 2013
© European Society of Radiology 2012

Abstract

Objectives To assess qualitative and quantitative chemical shift MRI parameters of renal cortical tumours.

Methods A total of 251 consecutive patients underwent 1.5-T MRI before nephrectomy. Two readers (R1, R2) independently evaluated all tumours visually for a decrease in signal intensity (SI) on opposed- compared with in-phase chemical shift images. In addition, SI was measured on in- and opposed-phase images (SI^{IP}, SI^{OP}) and the chemical shift index was calculated as a measure of percentage SI change. Histopathology served as the standard of reference.

Results A visual decrease in SI was identified significantly more often in clear cell renal cell carcinoma (RCCs) (R1, 73 %; R2, 64 %) and angiomyolipomas (both, 80 %) than in oncocytomas (29 %, 12 %), papillary (29 %, 17 %) and chromophobe RCCs (13 %, 9 %; all, $P < 0.05$). Median chemical shift index was significantly greater in clear cell RCC and angiomyolipoma than in the other histological subtypes (both, $P < 0.001$). Interobserver agreement was fair for visual (κ , 0.4) and excellent for quantitative analysis (concordance correlation coefficient, 0.80).

Conclusions A decrease in SI on opposed-phase chemical shift images is not an identifying feature of clear cell RCCs or angiomyolipomas, but can also be observed in oncocytomas, papillary and chromophobe RCCs. After excluding angiomyolipomas, a decrease in SI of more than 25 % was diagnostic for clear cell RCCs.

Key Points

- Chemical shift MRI offers new information about fat within renal tumours.
- Opposed-phase signal decrease can be observed in all renal cortical tumours.
- A greater than 25 % decrease in signal appears to be diagnostic for clear cell RCCs

Keywords Magnetic resonance imaging · Oncocytoma · Angiomyolipoma · Chemical shift imaging · Renal cell carcinoma

Introduction

Originally, evidence of fat within a renal cortical tumour on magnetic resonance imaging (MRI) was considered a unique, identifying feature of angiomyolipoma [1, 2]. However, further research soon revealed that renal cell carcinomas (RCCs) may also contain fat owing to lipid-producing tumour necrosis, bone metaplasia with fatty marrow elements, or entrapment of perinephric or renal sinus fat [3, 4]. Moreover—in addition to macroscopic fat—clear cell RCCs frequently contain varying amounts of intracellular lipid and glycogen [5–7], which can be visualized using chemical shift MRI [8, 9]. In chemical shift MRI, a decrease in signal intensity (SI) on opposed-phase gradient-echo images is a function of the ratio of lipid content to the total amount of tissue in each voxel. This produces effects in interfaces between fatty and watery tissue within each voxel, and in diffusely distributed fatty components in the corresponding voxels [10, 11]. In 1997, Outwater et al. [8] reported that clear cell RCCs may exhibit such a decrease in SI on opposed-phase when compared with in-phase chemical shift MR images and related this observation to the presence of intracellular lipid. In 1999, Yoshimitsu et al.

C. A. Karlo (✉) · O. F. Donati · I. A. Burger · H. Hricak · O. Akin
Department of Radiology,
Memorial Sloan-Kettering Cancer Center,
1275 York Avenue, Radiology Academic Offices, Room C278,
New York, NY 10065, USA
e-mail: karloc@mskcc.org

J. Zheng · C. S. Moskowitz
Department of Epidemiology and Biostatistics,
Memorial Sloan-Kettering Cancer Center, New York, NY, USA

[9] established a direct correlation between the histochemical proof of intracellular lipid and glycogen and a decrease in SI on opposed-phase compared with in-phase chemical shift MR images.

In 2010, Reuter and Tickoo [6] published a detailed report on the histopathological heterogeneity of renal cortical tumours and concluded that not all clear cell RCCs contain a preponderance of clear cells and that other renal cortical tumours may exhibit clear cell cytology as well. Therefore, our hypothesis was that—because of the histopathological heterogeneity of renal cortical tumours—a decrease in SI on opposed-phase chemical shift MR images might be encountered not only in clear cell RCCs and angiomyolipomas, but also in other benign and malignant renal cortical tumours. The objective of this study was to retrospectively investigate qualitative and quantitative chemical shift MR imaging parameters of clear cell, papillary and chromophobe RCC as well as angiomyolipomas and oncocytomas.

Materials and methods

Patients

The institutional review board approved this retrospective study and waived the informed consent requirement.

The inclusion criteria for this study were (i) total or partial nephrectomy between January 2005 and December 2010, performed at our institution; (ii) preoperative 1.5-T MRI of the abdomen, performed within the 90 days before surgery, and including transverse, chemical shift imaging sequences (in- and opposed-phase) as well as T1- and T2-weighted sequences available in DICOM format through our institution's PACS; (iii) histopathology reports confirming the diagnosis of clear cell RCC, chromophobe RCC, papillary RCC, oncocytoma or angiomyolipoma, as well as establishing the Fuhrman nuclear grade in the case of clear cell RCC. Finally, a total of 251 patients were eligible for study inclusion. The patients' demographic and tumour characteristics are summarised in Table 1.

Data acquisition

All MR imaging studies were performed on commercially available 1.5-T units (GE Medical Systems, Milwaukee, WI, USA [$n=214$]; Siemens Medical Solutions, Forchheim, Germany [$n=34$]; Philips Medical, Eindhoven, the Netherlands [$n=2$] and Toshiba Medical Systems Corp., Tokyo, Japan [$n=3$]). All MR imaging protocols included a transverse T1-weighted 2D dual-echo in-phase and opposed-phase sequence (repetition time/echo time, 102–375 ms/3.9–6.7 ms, 102–375 ms/1.8–4.7 ms; field of view, 36–44 cm; section

Table 1 Patient and tumour characteristics

Gender	Male	66.1 % (166/251)
	Female	33.9 % (85/251)
BMI	Median BMI (range)	28.4 (14.3–59.1)
Patient age	Median age (range), in years	59.0 (17–84)
Tumour type ^a	Clear cell RCC	70.7 % (179/253)
	Chromophobe RCC	9.1 % (23/253)
	Papillary RCC	9.5 (24/253)
	Oncocytoma	6.7 % (17/253)
	Angiomyolipoma	4 % (10/253)
Tumour size ^a	Median tumour size (range), in cm	4.5 (1–23)
Tumour side	Right	53 % (134/253)
	Left	47 % (119/253)
Tumour stage ^a	pT1a	39.1 % (95/243)
	pT1b	15.2 % (37/243)
	pT2a	4.1 % (10/243)
	pT2b	4.9 % (12/243)
	pT3a	12.8 % (31/243)
	pT3b	23.1 % (56/243)
	pT4	0.8 % (2/243)
Fuhrman nuclear grade ^b	1	2.8 % (5/179)
	2	44.2 % (79/179)
	3	37.9 % (68/179)
	4	15.1 % (27/179)

^a Histopathological data; tumour stage according to 6th edition of the American Joint Committee on Cancer (AJCC) cancer staging manual (available for all tumour types except angiomyolipoma)

^b For clear cell RCCs only

thickness, 7–8 mm; intersection gap, 1 mm; and matrix, 256×128). Median time span between the date of MRI and the date of surgery was 38 days (range, 1–90 days).

Data analysis

Blinded to histopathological information, two readers (O.D. and I.B.) independently performed all image analysis using commercially available DICOM post-processing software (Advantage WorkStation, GE). For tumour identification, both readers were allowed to review standard T1- and T2-weighted images. During image analysis, the corresponding in- and opposed-phase images were displayed simultaneously on the screens of the workstation. If a region of interest (ROI) was placed on an opposed-phase image in order to measure the SI, a cross-referencing tool automatically generated a matching ROI of the same size and same location on the corresponding in-phase image. Thus, signal intensities on in- and opposed-phase images were measured at the exact same tumour location. For each reader, image analysis involved the following sequence of steps. First, each tumour

was visually assessed on opposed-phase images for the presence of an area exhibiting a decrease in SI compared with the corresponding in-phase image. Then, if an area of SI decrease was identified, SI was measured within this area on in- and opposed-phase images. In addition to areas exhibiting a decrease in SI, both readers assessed each tumour for the presence of an area exhibiting an increase in SI on opposed-phase compared with the corresponding in-phase images. Then, if an area of SI increase was identified, SI was measured within this area on in- and opposed-phase images. If neither an area of increased nor an area of decreased SI could be identified, the result of the qualitative analysis was reported as “no change in SI”.

Statistical analysis

Continuous variables were expressed as medians and ranges, categorical variables as percentages and frequencies. All statistical analyses were performed using commercially available software (SPSS 19, IBM Corporation, Armonk, NY, USA; and SAS 9.2, SAS Institute, Cary, NC, USA). All tests were two-sided and a *P* value less than 0.05 was considered to indicate statistical significance. The standard of reference was surgical histopathology in all patients.

Serving as a measure of percentage difference in SI between in- and opposed phase images, the chemical shift index [12–14] was calculated: $[(SI^{OP} - SI^{IP})/SI^{IP}] \times 100\%$

Interobserver agreement regarding qualitative assessment was calculated using Cohen’s kappa and interpreted as follows: less than 0.20, poor agreement; 0.20–0.40, fair agreement; 0.40–0.60, moderate agreement; 0.60–0.80, strong agreement; and 0.80–1.00, excellent agreement [15]. Fisher’s exact test was used to examine whether qualitative chemical shift parameters (i.e. the presence of areas of decreasing or increasing SI) were distributed differently between different tumour types, separately for each reader.

Interobserver agreement regarding continuous variables (i.e. SI measurements) was calculated using the concordance correlation coefficient (ρ_c). The Kruskal–Wallis test and Wilcoxon rank-sum test were used to compare chemical shift index values between the different tumour types and between Fuhrman grades of clear cell RCC. The *P* values were adjusted using the Bonferroni method, separately for each reader.

Results

Histopathology

In 251 patients, histopathology identified 253 tumours (Table 1).

Interobserver agreement

Interobserver agreement for qualitative analysis of SI change between in- and opposed-phase images was fair ($\kappa=0.40$; 95 % CI, 0.32–0.69). Both readers concurred in the qualitative assessment in 64 % of tumours (162/253) and disagreed in 36 % (91/253).

Interobserver agreement for quantitative analysis of SI change between in- and opposed-phase images was excellent ($\rho_c=0.80$; 95 % CI, 0.75–0.86).

Qualitative results

Both readers detected areas of decreased SI on opposed-phase images significantly more often within clear cell RCCs and angiomyolipomas than within chromophobe RCCs, papillary RCCs or oncocytomas (R1, $P<0.001$; R2, $P=0.017$; Table 2; Figs. 1, 2 and 3).

Both readers detected areas of increased SI on opposed-phase images significantly more often within papillary RCCs, chromophobe RCCs and oncocytomas than within clear cell RCCs and angiomyolipomas (both readers, $P<0.001$; Table 2; Figs. 1, 2 and 3).

Quantitative results

Mean chemical shift index was significantly greater in clear cell RCCs than in all other histological tumour types (both readers, $P<0.001$; Fig. 4) except angiomyolipomas (R1, $P=1.0$; R2, $P=0.195$; Table 2). Mean chemical shift index did not differ significantly among Fuhrman grades of clear cell RCC (R1, $P=0.736$; R2, $P=0.418$). Mean chemical shift index was significantly greater in tumours for which readers’ qualitative assessments agreed (both readers, $P<0.001$; Table 3).

Discussion

The most important finding of this study was that areas of decreased SI on opposed-phase compared with in-phase chemical shift MR images were identified not only within clear cell RCCs and angiomyolipomas, but also within chromophobe RCCs, papillary RCCs and oncocytomas. Therefore, areas of decreased SI on opposed-phase images should not be considered a characteristic feature of clear cell RCCs or angiomyolipomas. However, when the change in SI between in- and opposed-phase was quantified, more than two thirds of clear cell RCCs exhibited a marked decrease in SI of more than 25 %. Thus, clear cell RCCs can be reliably differentiated from oncocytomas, papillary RCCs and chromophobe RCCs by the extent of SI decrease. Although angiomyolipomas displayed areas

Table 2 Summary of the results of the qualitative and quantitative analyses of signal intensity changes

Tumour type	Reader	SI decrease		SI increase		No change in SI <i>n</i>
		<i>n</i>	CSI	<i>n</i>	CSI	
Clear cell RCC	1	73 % (130/179)	22.9 (1.5–70.5)	18 % (32/179)	4.8 (5.6–66.1)	9 % (17/179)
	2	64 % (115/179)	22.2 (0.9–65.6)	8 % (14/179)	4.7 (11.5–40.3)	28 % (50/179)
Chromophobe RCC	1	13 % (3/23)	8.4 (5.2–10.3)	70 % (16/23)	3.4 (6.0–31.9)	17 % (4/23)
	2	9 % (2/23)	6.1 (4.2–8.0)	30 % (7/23)	8.3 (3.4–16.3)	61 % (14/23)
Papillary RCC	1	29 % (7/24)	8.0 (4.5–20.4)	58 % (14/24)	7.3 (6.5–66.1)	13 % (3/24)
	2	17 % (4/24)	11.6 (8.7–24.5)	46 % (11/24)	13.7 (0.6–60.3)	37 % (9/24)
Oncocytoma	1	29 % (5/17)	7.6 (2.7–15.0)	65 % (11/17)	1.5 (4.0–11.3)	6 % (1/17)
	2	12 % (2/17)	11.3 (8.1–14.5)	59 % (10/17)	5.5 (1.8–18.0)	29 % (5/17)
Angiomyolipoma	1	80 % (8/10)	38.4 (5.3–81.1)	10 % (1/10)	9.0	10 % (1/10)
	2	80 % (8/10)	45.6 (3.3–77.9)	10 % (1/10)	9.2	10 % (1/10)

CSI chemical shift index

of decreased SI more often (i.e. in 80 % of tumours) and more prominently (i.e. median chemical shift index >35 %) than any other histological tumour type, they could be correctly identified using typical MR imaging features such as the presence of macroscopic fat. Thus, after all angiomyolipomas were correctly identified, a decrease in

SI of more than 25 % was found to be diagnostic for clear cell RCCs.

A second important finding of our study was that the interreader agreement regarding the visual assessment of SI change was fair ($\kappa=0.4$), yielding that some areas of SI change were difficult to identify on opposed-phase

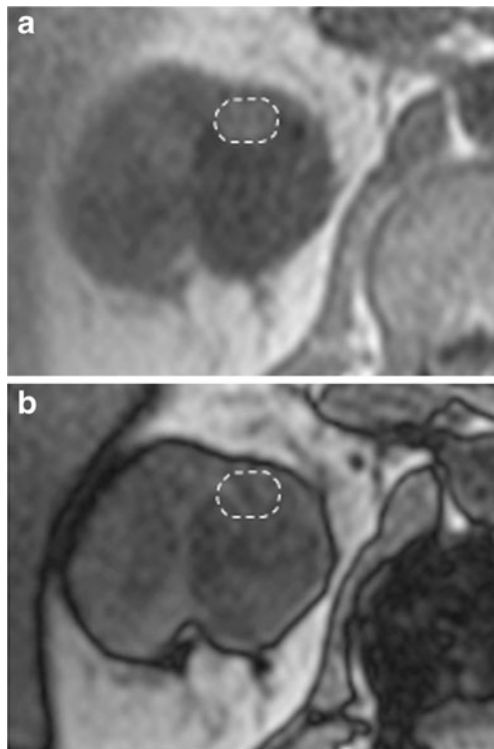


Fig. 1 Transverse in-phase (**a** TE, 4.2 ms) and opposed-phase (**b** TE, 1.8 ms) chemical shift 1.5-T MR images in a 56-year-old man with a clear cell carcinoma illustrating a solid tumour component (*dotted line*) that exhibits a decrease in signal intensity between the in-phase (**a**) and opposed-phase (**b**) images

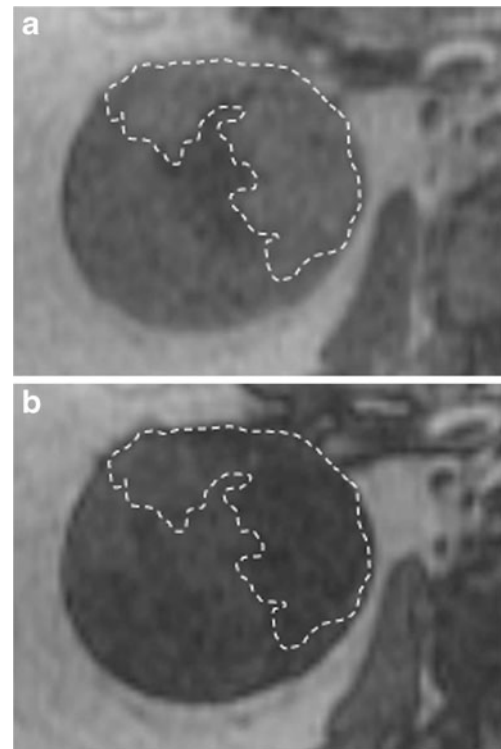


Fig. 2 Transverse in-phase (**a** TE, 4.2 ms) and opposed-phase (**b** TE, 2.0 ms) chemical shift 1.5-T MR images in a 51-year-old man with a clear cell carcinoma illustrating peripheral areas (*dotted line*) of hyperintense signal intensity on the in-phase (**a**) image markedly decreasing in signal intensity on the opposed-phase (**b**) image

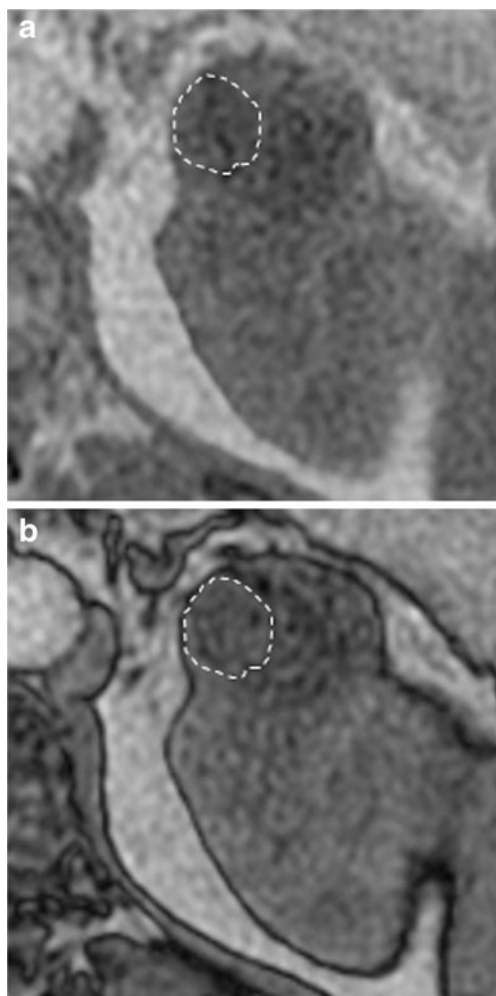


Fig. 3 Transverse in-phase (**a** TE, 4.2 ms) and opposed-phase (**b** TE, 2.0 ms) chemical shift 1.5-T MR images in a 71-year-old woman with clear cell carcinoma illustrating an increase in signal intensity from the in-phase (**a**) to the opposed-phase (**b**) image (*dotted line*)

images, as previously suggested [8]. However, the chemical shift index was greater in cases both readers agreed upon. Thus, the greater the decrease in SI on opposed-phase images, the easier it was to identify visually. Once identified, the measurement of SI on in- and opposed-phase images yielded good interreader agreement ($\rho_c=0.8$).

Outwater et al. [8], who were the first to describe the use of chemical shift MR imaging for the identification of intracellular lipid and glycogen within clear cell RCC cells, suggested that the presence of tumour areas exhibiting a decrease in SI on opposed-phase images was an identifying characteristic of angiomyolipomas and clear cell RCCs. Compared with their study, which included 27 clear cell RCCs, 3 oncocytomas and 1 angiomyolipoma along with a small number of other histological tumour types, we assessed a considerably larger number of tumours ($n=253$) and, more importantly, non-clear cell tumour types. Outwater et al. [8] reported one case of a

clear cell RCC that exhibited an area of increased SI on opposed-phase images and suggested that this might have been due to susceptibility caused by haemosiderin within intratumoural haemorrhage. In another study, Yoshimitsu et al. [16] observed that the presence of areas exhibiting an increased SI on opposed-phase images might be helpful in the identification of haemosiderin within papillary RCC. In our study, areas of increased SI on opposed-phase images were most common in papillary RCCs (>45 %), chromophobe RCCs (>30 %) and oncocytomas (>50 %), but were also identified in clear cell RCCs (<20 %) and angiomyolipomas (10 %). Therefore our results suggest that the presence of areas exhibiting an increase in SI on opposed-phase images should not be misinterpreted as an identifying characteristic of any histological type of renal cortical tumour investigated in this study.

Histopathology studies have shown that higher-grade clear cell RCCs (i.e. Fuhrman grades III and IV) contain less intracellular fat and lipid but larger areas of necrosis and intratumoural haemorrhage than do those of lower Fuhrman grades [6]. However, this finding was not reflected in our results, as chemical shift MR imaging findings did not differ significantly between low- and high-grade clear cell RCCs.

Our study has limitations. First, we retrospectively included chemical shift MRI studies acquired at 1.5 T only. Given that chemical shift MRI yields different data at higher field strengths [17], our results may not be directly applicable to examinations performed at other field strengths. In addition, the MRI studies included in this study were acquired using MRI machines from different vendors. However, the acquisition parameters of the chemical shift sequence were comparable. Second, the histopathology data that served as the standard of reference was derived from the institution's patient management system. The histopathology specimens were not re-analysed by a pathologist, which could have provided answers to additional questions such as the one oncocytoma that exhibited SI on opposed-phase images or the presence or absence of intratumoural haemorrhage. Moreover, an exact match-up between the focal areas of signal change within a tumour on imaging and the corresponding area on histopathology was not possible.

In conclusion, a decrease in SI on opposed-phase compared with in-phase chemical shift MR images is not a specific finding in clear cell RCCs and angiomyolipomas, but can be observed in oncocytomas, papillary RCCs and chromophobe RCCs. However, considering the fact that angiomyolipomas can be identified using characteristic MR imaging features, a decrease in SI of more than 25 % can be considered diagnostic of clear cell RCCs.

Fig. 4 Box and whisker plots (including 5th and 95th percentiles) demonstrating the change in signal intensity between in-phase and opposed-phase chemical shift MR images for all tumour types. The changes in signal intensity presented are the mean values of both readers

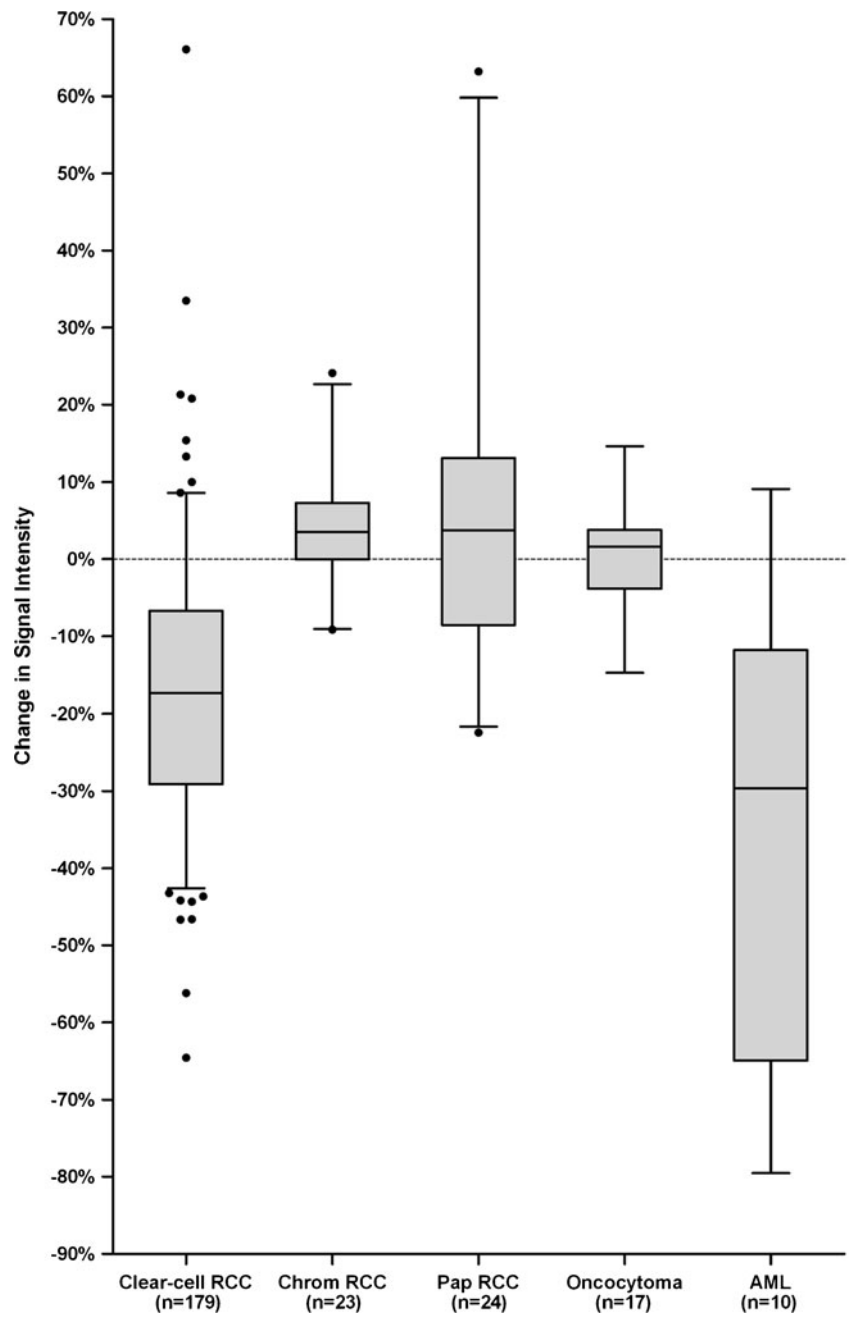


Table 3 Chemical shift index per reader regarding concurrent and non-concurrent qualitative assessment

	Both readers identified SI decrease n=116	One reader identified SI decrease n=15	Neither reader identified SI decrease n=33	P ^b
CSI (reader 1)	-24.5 (-81.1 to -3.4)	-7.8 (-46.6 to 24.3)	4.4 (-6.0 to 66.1)	<0.001
CSI (reader 2)	-23.0 (-77.9 to 0.9)	-8.4 (-29.8 to 35.0)	8.8 (-0.6 to 60.3)	<0.001
Tumour size ^a	4.8 (1.0 to 19.3)	3.5 (1.3 to 17.5)	5.0 (1.1 to 23.0)	0.514

CSI chemical shift index

^a Median tumour size in cm (range) as measured at histopathology

^b Significance of the difference in median CSI between tumours for which readers' qualitative assessments agreed and tumours for which readers' qualitative assessments disagreed

References

1. Kido T, Yamashita Y, Sumi S et al (1997) Chemical shift GRE MRI of renal angiomyolipoma. *J Comput Assist Tomogr* 21:268–270
2. Burdeny DA, Semelka RC, Kelekis NL, Reinhold C, Ascher SM (1997) Small (<1.5 cm) angiomyolipomas of the kidney: characterization by the combined use of in-phase and fat-attenuated MR techniques. *Magn Reson Imaging* 15:141–145
3. Israel GM, Hindman N, Hecht E, Krinsky G (2005) The use of opposed-phase chemical shift MRI in the diagnosis of renal angiomyolipomas. *AJR Am J Roentgenol* 184:1868–1872
4. Kim JK, Kim SH, Jang YJ et al (2006) Renal angiomyolipoma with minimal fat: differentiation from other neoplasms at double-echo chemical shift FLASH MR imaging. *Radiology* 239:174–180
5. Reuter VE (2006) The pathology of renal epithelial neoplasms. *Semin Oncol* 33:534–543
6. Reuter VE, Tickoo SK (2010) Differential diagnosis of renal tumours with clear cell histology. *Pathology* 42:374–383
7. Tickoo SK, Gopalan A (2008) Pathologic features of renal cortical tumors. *Urol Clin North Am* 35:551–561
8. Outwater EK, Bhatia M, Siegelman ES, Burke MA, Mitchell DG (1997) Lipid in renal clear cell carcinoma: detection on opposed-phase gradient-echo MR images. *Radiology* 205:103–107
9. Yoshimitsu K, Honda H, Kuroiwa T et al (1999) MR detection of cytoplasmic fat in clear cell renal cell carcinoma utilizing chemical shift gradient-echo imaging. *J Magn Reson Imaging* 9:579–585
10. Mitchell DG, Kim I, Chang TS et al (1991) Fatty liver. Chemical shift phase-difference and suppression magnetic resonance imaging techniques in animals, phantoms, and humans. *Invest Radiol* 26:1041–1052
11. Mitchell DG, Crovello M, Matteucci T, Petersen RO, Miettinen MM (1992) Benign adrenocortical masses: diagnosis with chemical shift MR imaging. *Radiology* 185:345–351
12. Fujiyoshi F, Nakajo M, Fukukura Y, Tsuchimochi S (2003) Characterization of adrenal tumors by chemical shift fast low-angle shot MR imaging: comparison of four methods of quantitative evaluation. *AJR Am J Roentgenol* 180:1649–1657
13. Jacques AE, Sahdev A, Sandrasagara M et al (2008) Adrenal pheochromocytoma: correlation of MRI appearances with histology and function. *Eur Radiol* 18:2885–2892
14. Siegelman ES (2012) Adrenal MRI: techniques and clinical applications. *J Magn Reson Imaging* 36:272–285
15. Landis JR, Koch GG (1977) The measurement of observer agreement for categorical data. *Biometrics* 33:159–174
16. Yoshimitsu K, Kakihara D, Irie H et al (2006) Papillary renal carcinoma: diagnostic approach by chemical shift gradient-echo and echo-planar MR imaging. *J Magn Reson Imaging* 23:339–344
17. Nakamura S, Namimoto T, Morita K et al (2012) Characterization of adrenal lesions using chemical shift MRI: comparison between 1.5 tesla and two echo time pair selection at 3.0 tesla MRI. *J Magn Reson Imaging* 35:95–102